ENA periodicities and their phase relations to SKR emissions at Saturn

J. F. Carbary,[1] D. G. Mitchell,[1] P. C. Brandt,[1] S. M. Krimigis,[1] and D. A. Gurnett[2]

Received 8 June 2011; revised 19 July 2011; accepted 20 July 2011; published 24 August 2011.

[1] Cassini orbits during days 200–366 in 2004 afforded the opportunity to continuously observe energetic neutral atom (ENA) emissions from long range (>50 R_S, 1 R_S = 60268 km) on Saturn's dawn side. Images of energetic neutral hydrogen (25–55 keV) and oxygen (90–160 keV) were projected onto the noon-midnight plane, corrected for travel time from Saturn, averaged into half hour time bins and finally averaged into a 60 × 40 R_S spatial bin. The time profiles of these bin averages were then subjected to a Lomb periodogram analysis. The H periodogram exhibits a weak periodicity (SNR = 9.1) with a major peak at 10.78 hours and several minor peaks. The O periodogram displays strong periodicities (SNR = 36.2) with a major peak at 10.78 hours and a various secondary peaks. A cross correlation of the SKR signal with the ENA signals reveals that the H signal leads the SKR by 1.46 ± 0.08 hours, while the O signal leads the SKR by 2.21 ± 0.14 hours. **Citation:** Carbary, J. F., D. G. Mitchell, P. C. Brandt, S. M. Krimigis, and D. A. Gurnett (2011), ENA periodicities and their phase relations to SKR emissions at Saturn, *Geophys. Res. Lett.*, *38*, L16106, doi:10.1029/2011GL048418.

1. Introduction

[2] A variety of magnetospheric and ionospheric phenomena at Saturn exhibit periodicities near 10.8 hours. Foremost among these periodic phenomena is the Saturn kilometric radiation (SKR), which Voyager observations showed had a period near 10.66 hours [*Desch and Kaiser*, 1981]. Later SKR measurements by the Ulysses and Cassini spacecraft showed that the SKR period had evolved to 10.71 hours by 1997 [*Galopeau and Lecacheux*, 2000] and to 10.76 hours by 2004 [*Gurnett et al.*, 2005]. Variations in the radio period could actually be tracked, which led to the establishment of "variable" longitude systems [*Kurth et al.*, 2007, 2008]. Cassini observations later discovered a second, shorter SKR period; the longer SKR period was associated with a source in the southern hemisphere and the shorter SKR period was associated with a northern source [*Gurnett et al.*, 2009]. Extensive monitoring of both sources revealed that both the north and south periods slowly changed, so much so that they "reversed" shortly after Saturn's equinox in 2009 [*Gurnett et al.*, 2010].

[3] Additional periodicities near or at the SKR periods have been found in charged particles [*Carbary and Krimigis*, 1982; *Carbary et al.*, 2007], magnetic fields [*Espinosa and Dougherty*, 2000; *Giampieri et al.*, 2006], and energetic neutral atoms [*Paranicas et al.*, 2005; *Carbary et al.*, 2008a]. Oscillations at the SKR period have been detected in plasma sheet [*Carbary et al.*, 2008b], aurora [*Nichols et al.*, 2008], magnetopause [*Clarke et al.*, 2006], and even bow shock [*Clarke et al.*, 2010].

[4] The frequency match between so many magnetospheric phenomena and the SKR encourages investigation of the phase relation between these phenomena and the radio emissions. Oscillations of the equatorial and high latitude perturbation magnetic fields have been thoroughly examined by measuring their phase relations with the SKR oscillations [*Andrews et al.*, 2008, 2010; *Provan et al.*, 2009]. The oscillations of components of the perturbation magnetic field generally follow the SKR phase, albeit they have important shifts in radial distance and local time. Saturn's UV aurora emissions peak at the same time as the SKR power, at least on the dawnside, so the aurora seems to be in phase with SKR [*Nichols et al.*, 2010]. Bursts of energetic neutral atoms (ENA) and SKR closely correspond [*Mitchell et al.*, 2009], although statistically the ENA-SKR phases are not consistent on short time scales of days [*Carbary et al.*, 2010].

[5] Being produced by charge exchange between energetic ions and cold neutrals, the ENA fluxes offer a direct, global measurement of magnetospheric oscillations and effectively serve as a proxy for energetic ion fluxes. The phase of the ENA oscillations relative to the SKR is of immediate interest because of a possible causal relation between magnetospheric phenomena and radio phenomena. The ENA-SKR phases have so far been investigated in a limited fashion using only a few case studies. After first checking the ENA periodicities, this study formally correlates the ENA and SKR phases over 167 days during 2004 and deduces a statistical relation between the two.

2. Data and Data Processing

[6] The Ion-Neutral CAmera (INCA), which is part of the Magnetospheric IMaging Instrument (MIMI) on the Cassini spacecraft, measures energetic neutral atoms. Details of the instrument and data processing appear elsewhere [e.g., *Krimigis et al.*, 2004; *Carbary et al.*, 2008a]. This study relies on fluxes of neutral hydrogen atoms (25–55 kev) and neutral oxygen atoms (90–160 keV) that were observed from days 200 to 366 in 2004. This period was used because the ENA data are essentially continuous, because the long ranges from Saturn ensure complete coverage of the magnetosphere, and because spacecraft maneuvers did not disrupt the views of Saturn. Figure 1 (left) shows the Cassini trajectory for the 167 days of coverage studied here.

[7] The energetic H atoms travel at ~2600 km/s and the energetic O atoms travel at ~1200 km/s, so they require tens of minutes to travel from Saturn to Cassini at the ranges of

[1]Johns Hopkins University Applied Physics Laboratory, Laurel, Maryland, USA.
[2]Department of Physics and Astronomy, University of Iowa, Iowa City, Iowa, USA.

0094-8276/11/2011GL048418

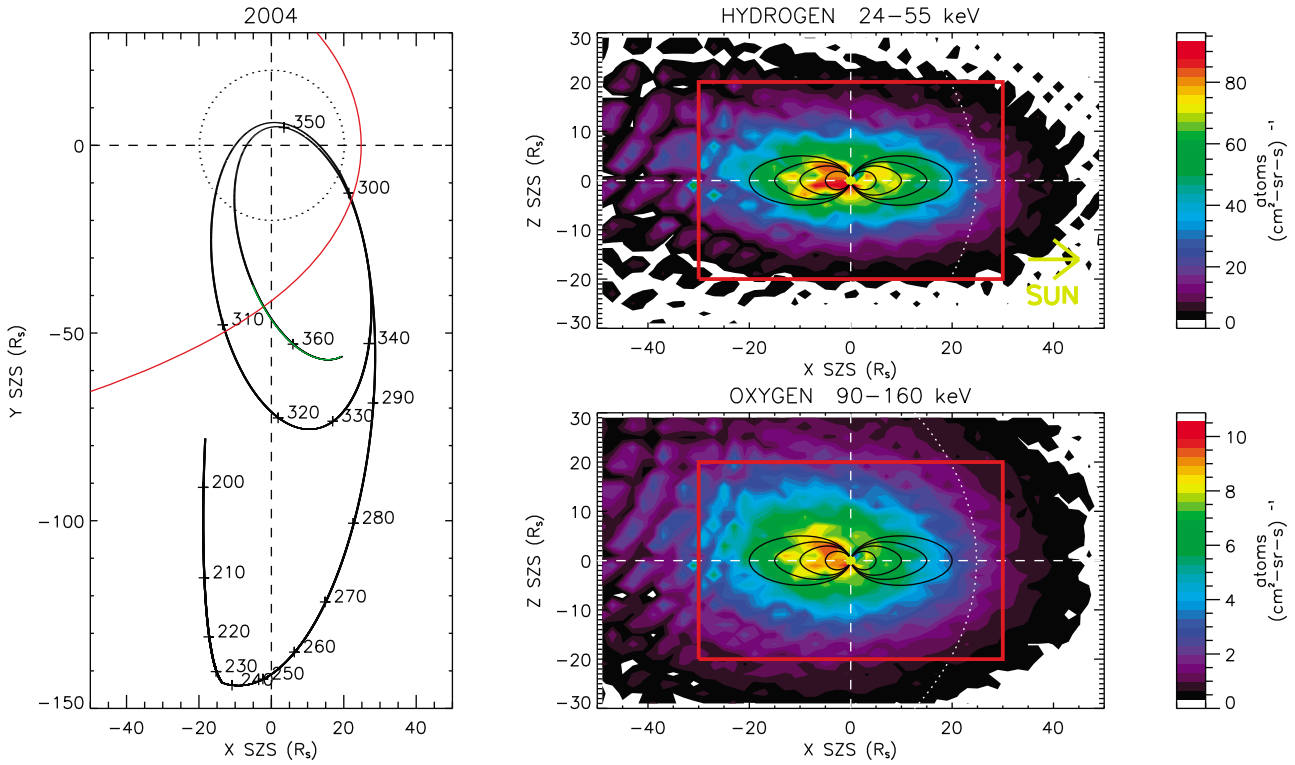

Figure 1. (left) Trajectory of Cassini from days 200–366 in 2004 and composite images of (top right) energetic hydrogens and (bottom right) energetic oxygens from days 355–366 in 2004. In the trajectory plot, the observer looks down from the north pole of Saturn, and the Sun is to the right. The red curve indicates an approximate magnetopause, the dotted circle shows the orbit of Titan, and the green trajectory segment shows that period from which the composites were assembled. The composites represent flux averages into 2 × 2 R_S bins over the 12 days in 2004. The composite images are projections onto the noon-midnight plane of Saturn; the red boxes denote regions over which the projected fluxes were averaged to determine time profiles.

observation (only Cassini ranges greater than 30 R_S were employed). The time marks of the INCA images were corrected for the travel times of each species of particle using the geometric means of the energy ranges. To improve statistics, the ENA fluxes from individual INCA images were then time-averaged on a pixel-by-pixel basis into half-hour bins. The average pointing was next used to project the fluxes onto the noon-midnight plane of Saturn by finding the pierce points of the pixels on this plane. Time profiles of the ENA fluxes were finally calculated by averaging all pixels falling within 60 × 40 R_S boxes centered on Saturn. Figure 1 (right) illustrate these averaging boxes and how they encompass the ENA emissions coming from Saturn's magnetosphere. A complete discussion of the projection geometry and box averaging has been given before [*Carbary et al.*, 2008a]. Average projected range errors of ~0.8% arise from assuming all the ENA fluxes originate at Saturn, while particle speed errors of ~1–2% arise from using the geometric mean of ENA energies rather than an energy based on the ENA spectrum, which is any case is imperfectly known [*Carbary et al.*, 2008c]. Adding these uncertainties in quadrature amounts to travel times having errors of ~2.3% for hydrogen ENA and ~1.4% for oxygen ENA.

[8] The time profile of SKR emissions is obtained from the electric field strengths observed by the Radio Plasma Wave Science (RPWS) instrument on Cassini [*Gurnett et al.*, 2004]. The field vectors were integrated over the kilometric band from 100 to 400 kHz and also averaged to half hour time resolution for compatibility with the ENA signal. The SKR data were not adjusted for travel time because the radio waves move at the speed of light and travel times are negligible.

[9] Figure 2 (top and middle) compares box-averaged time profiles from hydrogen and oxygen ENA with the time profile of SKR (Figure 2, bottom). These profiles represent a subset of 31 days out of the 167 days using in the full study. The ENA profiles look remarkably similar to each other although they differ in magnitude. At first glance, the SKR profile seems dissimilar to those of the ENA, although more scrutiny reveals a similarity between the ENA and radio signals. In particular, the "bursts" on days 324 and 338 appear in all the profiles. Also, note that numerous gaps appear in the ENA profiles. These are generally caused by spacecraft maneuvers that shift the field of view away from Saturn. The SKR record contains many fewer gaps. Finally, large-scale variations in the ENA occur at irregular time intervals of 5–10 days. These variations are probably caused by solar wind disturbances acting on the magnetosphere. While important, such disturbances are not the subject of this investigation and will be discussed in another paper.

3. ENA Periodicity

[10] Before conducting a formal cross correlation between the ENA and SKR signals, a Lomb periodogram analysis is

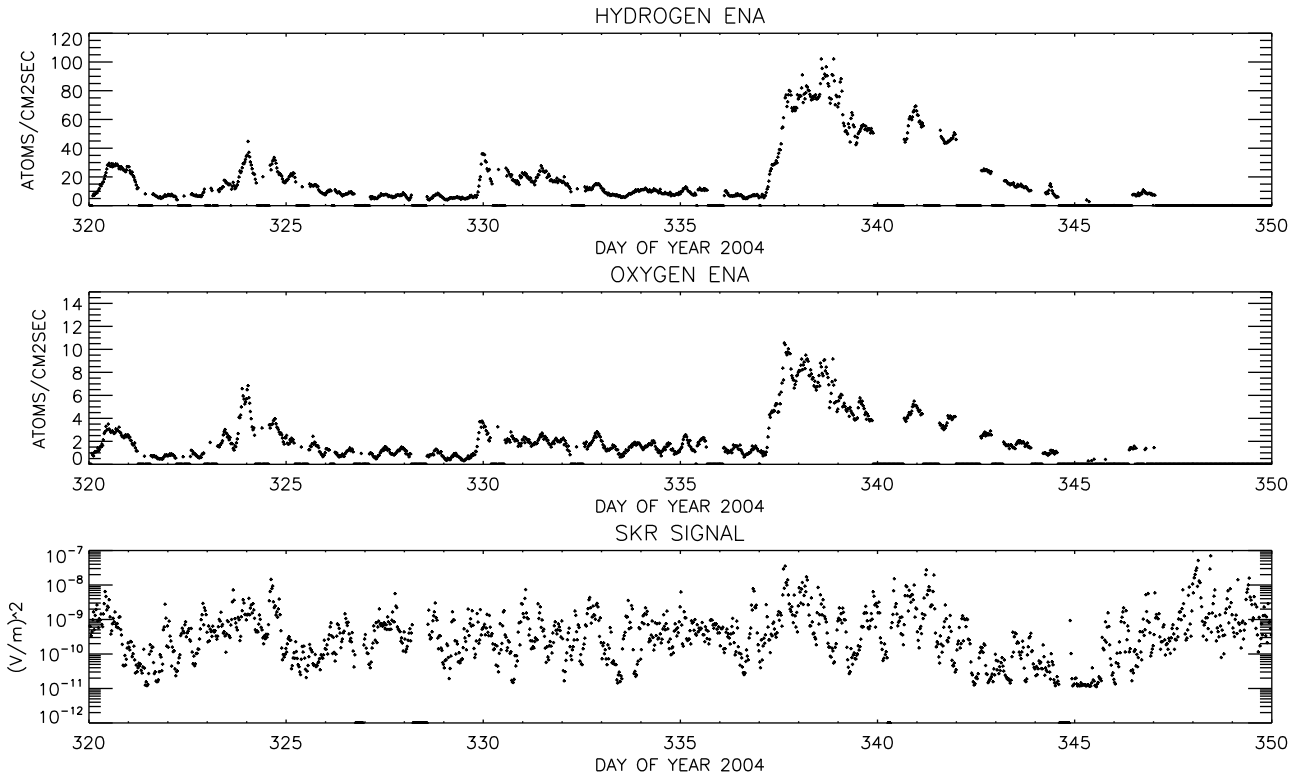

Figure 2. Sample time profiles of the (top) hydrogen, (middle) oxygen, and (bottom) SKR emissions for 30 days in 2004. The ENA emissions are half-hour averages of ENA fluxes within 60 × 40 R_S boxes centered on Saturn, while the SKR emissions are half-hour averages from 100 to 400 kHz from the RPWS instrument. The times of the ENA fluxes were corrected for time-of-flight from Saturn to the spacecraft.

conducted to verify the ENA periods and show they are the same as that of the SKR. The establishment of phase relations between two signals requires that they share a common frequency.

[11] Figure 3 displays periodograms for the neutral H (Figure 3, top) and neutral O (Figure 3, bottom) and clearly demonstrates the principal periods of both signals are exactly those of the SKR at this time, namely, 10.78 hours [e.g., *Gurnett et al.*, 2009]. The H signal appears weaker and noisier than the O signal; this has been recognized in previous examinations of the ENA spectra [*Carbary et al.*, 2008a]. The periodograms also reveal secondary signals that have statistical significance but are not relevant to the correlations. The sources of these signals are unknown, but may be related to solar wind modulations known to affect the radio emissions [e.g., *Zarka et al.*, 2007]. Alternately, they may be rotational signals unrelated to the SKR. A weak signal also appears at 10.61 hours in the oxygen periodogram, and this might represent the beginning of a dual periodicity in the ENA. At this epoch, however, the SKR signal is primarily that of the southern source with a period near 10.78 hours [*Gurnett et al.*, 2009]. This 10.78 hour period is the principal correlative for the ENA and SKR signals.

4. Cross Correlation and Discussion

[12] Figure 4 presents the formal cross correlations between the ENA signals and the logarithm of the SKR signal, and shows how they differ from two random signals of the same resolution and duration. The linear cross correlation coefficient between the time profiles has been used; gaps in each signal were carefully accounted for and removed. For both species of ENA, the SKR signal lags the ENA signal. The peak cross correlation of the SKR is stronger for the oxygen ENA (~0.56) than for the hydrogen ENA (~0.45). The weaker H correlation strength probably results from the noisier hydrogen signal. The hydrogen ENA signal leads the SKR signal by 1.46 ± 0.08 hours, while the oxygen ENA leads the SKR by 2.21 ± 0.14 hours, where the uncertainties are those of the cross correlation peak. The differing lead times may have to do with the faster drift times for energetic oxygen ions compared to protons. Recall that the ENA is essentially a proxy for energetic ions that generate ENA through charge exchange.

[13] The ENA signals represent a global measure of magnetospheric activity, as might be expected from the ring current. The phase relations of both the hydrogen and oxygen ENA relative to SKR suggest that magnetospheric activity precedes radio activity, and by time periods of one to three hours. Some care should be exercised in accepting this interpretation, because the intensity of both the SKR and ENA signals varies with location, so the exact phasing might be biased by observer location. The ENA emissions appear to maximize in the midnight sector and move counter-clockwise around Saturn [*Carbary et al.*, 2008c], while the SKR emissions are predominant in the morning to noon local time

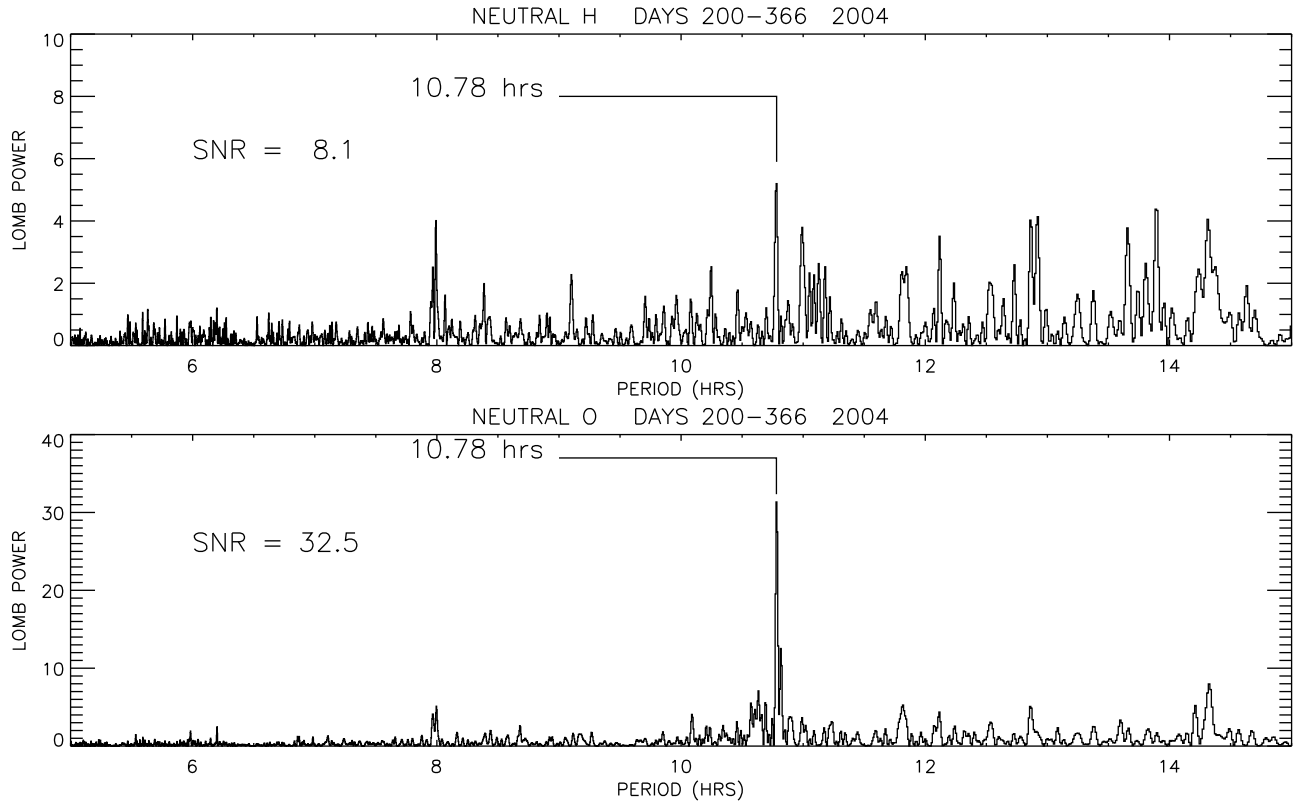

Figure 3. Lomb periodograms of (top) neutral hydrogen and (bottom) neutral oxygen. SNR refers to the signal-to-noise ratio of the peak emission to the average of the other peaks in the 5–15 hour window examined here.

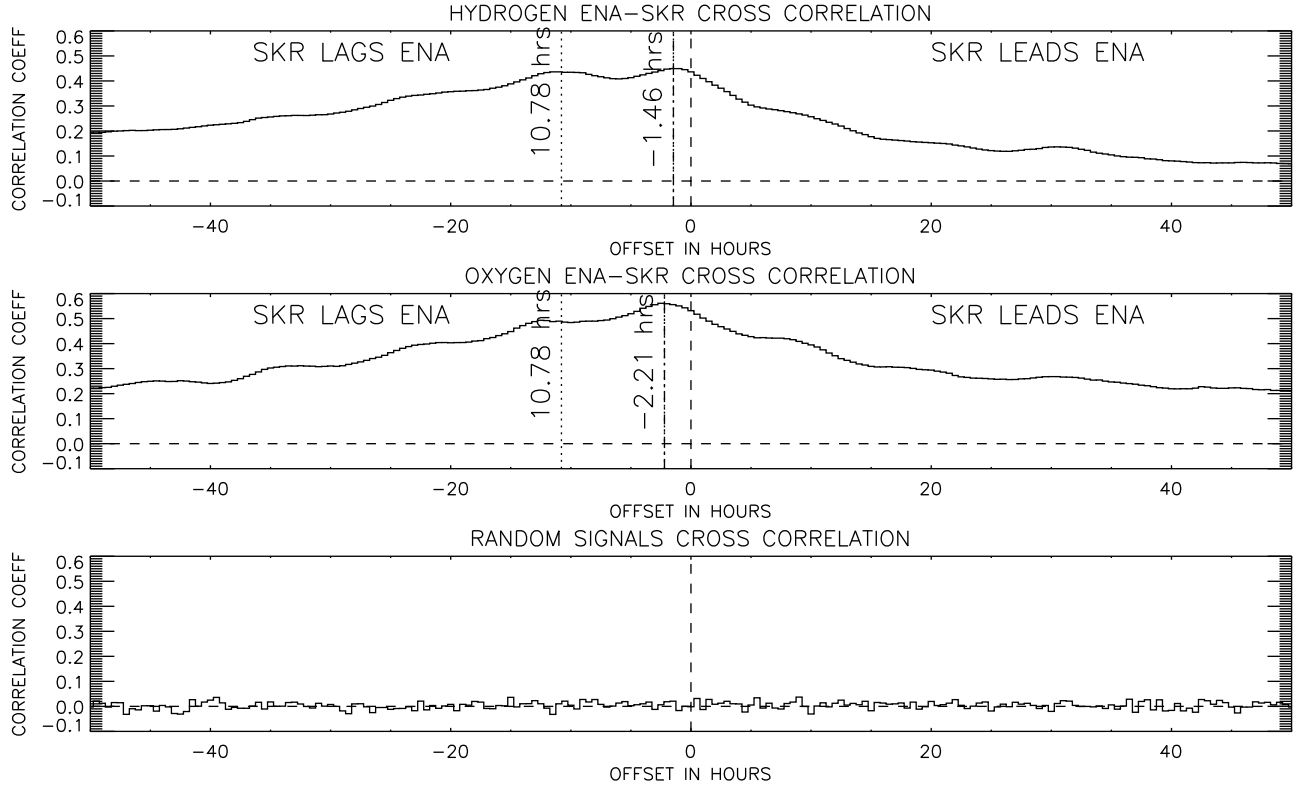

Figure 4. Cross correlations between (top) hydrogen ENA and SKR and (middle) oxygen ENA and SKR. The cross correlation peaks are denoted with vertical dot-dash lines, while the main 10.78 period is indicated with dotted lines. (bottom) The cross correlation between two random signals having the same number of samples and time resolution as the ENA-SKR observations.

sectors [*Lamy et al.*, 2008; *Cecconi et al.*, 2009]. For the data used herein, the observer had a stationary location on the dawn flank of Saturn.

[14] The magnetospheric ENA activity precedes the radio activity in time, so one may infer that it generates or drives the radio activity. The following scenario may be envisioned. The ENA modulation results from a rotating source or "blob" that intensifies or originates near midnight, so a dawnside observer would first see an ENA enhancement on the nightside. This enhancement would then sweep eastwards to the dayside, activating the dawn-to-noon radio emissions as it does so. The different lead times of the hydrogen and oxygen relative to the SKR result from different ion drift speeds and/or different activation locations for the two species. Pressure gradients associated with the ENA blob would drive currents responsible for SKR emissions as well as magnetic field oscillations.

[15] A previous study of ENA-SKR interpreted their phase differences in terms of clocks having the same periods and being re-set by external effects [*Carbary et al.*, 2010]. This earlier hypothesis may still have merit, although it was based on a limited number of case studies and using equatorial (rather than noon-midnight) projections. Spanning a longer time interval, the present study finds no evidence for re-setting of the ENA clocks relative to SKR.

5. Conclusions

[16] ENA emissions were observed from the Cassini spacecraft on the dawn side of Saturn for 167 days in 2004. After correction for travel time from Saturn and projection onto the noon-midnight plane, the ENA fluxes were averaged into half hour time bins and then into a 60 × 40 R_S spatial bin to generate a time profile of the emissions. Lomb spectra of both the hydrogen and oxygen ENA exhibit strong periodicities at the 10.78 period of the Saturn kilometric radiation (100–400 kHz) seen during the same interval. A cross correlation of the SKR signal with the ENA signals shows that the H signal leads the SKR by 1.46 ± 0.08 hours, while the O signal leads the SKR by 2.21 ± 0.14 hours. Because these magnetospheric ENA signals always lead the ionospheric SKR signal, one infers a magnetospheric driver, marked by the ENA source, that rotates from midnight through dawn to noon and triggers SKR emissions as it does.

[17] **Acknowledgments.** This research was supported in part by the NASA Office of Space Science under task order 003 of contract NAS5-97271 between NASA Goddard Space flight Center and the Johns Hopkins University.

[18] The Editor wishes to acknowledge Anna DeJong and an anonymous reviewer for their assistance evaluating this paper.

References

Andrews, D. J., E. J. Bunce, S. W. H. Cowley, M. K. Dougherty, G. Provan, and D. J. Southwood (2008), Planetary spin period oscillations in Saturn's magnetosphere: Phase relations of equatorial magnetic field oscillations and SKR modulation, *J. Geophys. Res.*, *113*, A09205, doi:10.1029/2007JA012937.

Andrews, D. J., S. W. H. Cowley, M. K. Dougherty, and G. Provan (2010), Magnetic field oscillations near the planetary period in Saturn's equatorial magnetosphere: Variation of amplitude and phase with radial distance and time, *J. Geophys. Res.*, *115*, A04212, doi:10.1029/2009JA014729.

Carbary, J. F., and S. M. Krimigis (1982), Charged particle periodicity in the Saturnian magnetosphere, *Geophys. Res. Lett.*, *9*, 1073–1076, doi:10.1029/GL009i009p01073.

Carbary, J. F., D. G. Mitchell, S. M. Krimigis, D. C. Hamilton, and N. Krupp (2007), Charged particle periodicities in Saturn's outer magnetosphere, *J. Geophys. Res.*, *112*, A06246, doi:10.1029/2007JA012351.

Carbary, J. F., D. G. Mitchell, P. Brandt, C. Paranicas, and S. M. Krimigis (2008a), ENA periodicities at Saturn, *Geophys. Res. Lett.*, *35*, L07102, doi:10.1029/2008GL033230.

Carbary, J. F., D. G. Mitchell, P. Brandt, E. C. Roelof, and S. M. Krimigis (2008b), Periodic tilting of Saturn's plasma sheet, *Geophys. Res. Lett.*, *35*, L24101, doi:10.1029/2008GL036339.

Carbary, J. F., D. G. Mitchell, P. Brandt, E. C. Roelof, and S. M. Krimigis (2008c), Statistical morphology of ENA emissions at Saturn, *J. Geophys. Res.*, *113*, A05210, doi:10.1029/2007JA012873.

Carbary, J. F., D. G. Mitchell, S. M. Krimigis, D. A. Gurnett, and W. S. Kurth (2010), Phase relations between energetic neutral atom intensities and kilometric radio emissions at Saturn, *J. Geophys. Res.*, *115*, A01203, doi:10.1029/2009JA014519.

Cecconi, B., L. Lamy, R. Prangé, W. S. Kurth, and P. Louarn (2009), Goniopolarimetric study of the revolution 29 perikrone using the Cassini Radio and Plasma Wave Science instrument high-frequency radio receiver, *J. Geophys. Res.*, *114*, A03215, doi:10.1029/2008JA013830.

Clarke, K. E., et al. (2006), Cassini observations of planetary-period oscillations of Saturn's magnetopause, *Geophys. Res. Lett.*, *33*, L23104, doi:10.1029/2006GL027821.

Clarke, K. E., D. J. Andrews, A. J. Coates, S. W. H. Cowley, and A. Masters (2010), Magnetospheric period oscillations of Saturn's bow shock, *J. Geophys. Res.*, *115*, A05202, doi:10.1029/2009JA015164.

Desch, M. D., and M. L. Kaiser (1981), Voyager measurements of the rotation period of Saturn's magnetic field, *Geophys. Res. Lett.*, *8*, 253–256, doi:10.1029/GL008i003p00253.

Espinosa, S. A., and M. K. Dougherty (2000), Periodic perturbations in Saturn's magnetic field, *Geophys. Res. Lett.*, *27*, 2785–2788, doi:10.1029/2000GL000048.

Galopeau, P. H. M., and A. Lecacheux (2000), Variations in Saturn's radio period measured at kilometer wavelengths, *J. Geophys. Res.*, *105*, 13,089–13,101, doi:10.1029/1999JA005089.

Giampieri, G., M. K. Dougherty, E. J. Smith, and C. T. Russell (2006), A regular period for Saturn's magnetic field that may track its internal rotation, *Nature*, *441*, 62–64, doi:10.1038/nature04750.

Gurnett, D. A., et al. (2004), The Cassini radio and plasma wave investigation, *Space Sci. Rev.*, *114*, 395–463, doi:10.1007/s11214-004-1434-0.

Gurnett, D. A., et al. (2005), Radio and plasma wave observations at Saturn from Cassini's approach and first orbit, *Science*, *307*, 1255–1259, doi:10.1126/science.1105356.

Gurnett, D. A., A. Lecacheux, W. S. Kurth, A. M. Persoon, J. B. Groene, L. Lamy, P. Zarka, and J. F. Carbary (2009), Discovery of a north-south asymmetry in Saturn's radio rotation period, *Geophys. Res. Lett.*, *36*, L16102, doi:10.1029/2009GL039621.

Gurnett, D. A., J. B. Groene, A. M. Persoon, J. D. Menietti, S.-Y. Ye, W. S. Kurth, R. J. MacDowall, and A. Lecacheux (2010), The reversal of the rotational modulation rates of the north and south components of Saturn kilometric radiation near equinox, *Geophys. Res. Lett.*, *37*, L24101, doi:10.1029/2010GL045796.

Krimigis, S. M., et al. (2004), Magnetosphere Imaging Instrument (MIMI) on the Cassini mission to Saturn/Titan, *Space Sci. Rev.*, *114*, 233–329, doi:10.1007/s11214-004-1410-8.

Kurth, W. S., A. Lecacheux, T. F. Averkamp, J. B. Groene, and D. A. Gurnett (2007), A Saturnian longitude system based on a variable kilometric radiation period, *Geophys. Res. Lett.*, *34*, L02201, doi:10.1029/2006GL028336.

Kurth, W. S., T. F. Averkamp, D. A. Gurnett, J. B. Groene, and A. Lecacheux (2008), An update to a Saturnian longitude system based on kilometric radio emissions, *J. Geophys. Res.*, *113*, A05222, doi:10.1029/2007JA012861.

Lamy, L., P. Zarka, R. Prang, W. S. Kurth, and D. A. Gurnett (2008), Saturn kilometric radiation: Average and statistical properties, *J. Geophys. Res.*, *113*, A07201, doi:10.1029/2007JA012900.

Mitchell, D. G., et al. (2009), Recurrent energization of plasma in the midnight-to-dawn quadrant of Saturn's magnetosphere, and its relationship to auroral UV and radio emissions, *Planet. Space Sci.*, *57*, 1732–1742, doi:10.1016/j.pss.2009.04.002.

Nichols, J. D., J. T. Clarke, S. W. H. Crowley, J. Duval, A. J. Farmer, J.-C. Gérard, D. Grodent, and S. Wannawichian (2008), Oscillation of Saturn's southern auroral oval, *J. Geophys. Res.*, *113*, A11205, doi:10.1029/2008JA013444.

Nichols, J. D., B. Cecconi, L. T. Clarke, S. W. H. Cowley, J.-C. Gérard, A. Grocott, D. Grodent, L. Lamy, and P. Zarka (2010), Variation of Saturn's UV aurora with SKR phase, *Geophys. Res. Lett.*, *37*, L15102, doi:10.1029/2010GL044057.

Paranicas, C., D. G. Mitchell, E. C. Roelof, P. C. Brandt, D. J. Williams, S. M. Krimigis, and B. H. Mauk (2005), Periodic intensity variations in global ENA images of Saturn, *Geophys. Res. Lett.*, *32*, L21101, doi:10.1029/2005GL023656.

Provan, G., D. J. Andrews, C. S. Arridge, S. W. H. Cowley, S. E. Milan, M. K. Dougherty, and D. M. Wright (2009), Polarization and phase of planetary period oscillations on high latitude field lines in Saturn's magnetosphere, *J. Geophys. Res.*, *114*, A02225, doi:10.1029/2008JA013782.

Zarka, P., L. Lamy, B. Cecconi, and R. Prangé (2007), Modulation of Saturn's radio clock by solar wind speed, *Nature*, *450*, 265–267, doi:10.1038/nature06237.

P. C. Brandt, J. F. Carbary, S. M. Krimigis, and D. G. Mitchell, Johns Hopkins University Applied Physics Laboratory, 11100 Johns Hopkins Rd., Laurel, MD 20723-6099, USA. (james.carbary@jhuapl.edu)

D. A. Gurnett, Department of Physics and Astronomy, University of Iowa, Iowa City, IA 52242-1479, USA.